

Separate Mechanisms for Perception of Numerosity and Density

Giovanni Anobile¹, Guido Marco Cicchini², and David C. Burr^{1,2}

¹Department of Neuroscience, Psychology, Pharmacology, and Child Health, University of Florence, and ²Neuroscience Institute, National Research Council, Pisa, Italy

Psychological Science
2014, Vol. 25(1) 265–270
© The Author(s) 2013
Reprints and permissions:
sagepub.com/journalsPermissions.nav
DOI: 10.1177/0956797613501520
pss.sagepub.com
SAGE

Abstract

Despite the existence of much evidence for a number sense in humans, several researchers have questioned whether number is sensed directly or derived indirectly from texture density. Here, we provide clear evidence that numerosity and density judgments are subserved by distinct mechanisms with different psychophysical characteristics. We measured sensitivity for numerosity discrimination over a wide range of numerosities: For low densities (less than 0.25 dots/deg²), thresholds increased directly with numerosity, following Weber's law; for higher densities, thresholds increased with the square root of texture density, a steady decrease in the Weber fraction. The existence of two different psychophysical systems is inconsistent with a model in which number is derived indirectly from noisy estimates of density and area; rather, it points to the existence of separate mechanisms for estimating density and number. These results provide strong confirmation for the existence of neural mechanisms that sense number directly, rather than indirectly from texture density.

Keywords

perception, visual perception, number comprehension

Received 1/30/13; Revision accepted 7/23/13

Much physiological and psychophysical research suggests that humans (including infants) share with many animals a number sense (i.e., the ability to estimate rapidly the approximate number of items in a scene; Burr & Ross, 2008a; Dehaene, 1997; Nieder, 2005). However, several researchers have questioned whether number is in fact sensed directly, suggesting instead that it can be derived only indirectly from texture density (Burr & Ross, 2008b; Dakin, Tibber, Greenwood, Kingdom, & Morgan, 2011; Durgin, 2008). In this study, we measured Weber fractions for numerosity and density discrimination as a function of dot density, and we found that different mechanisms are involved at high and low densities.

Method

We measured thresholds for discriminating numerosity and density of two clouds of nonoverlapping dots confined to circular regions on either side of a central fixation point (Fig. 1a). The numerosity of the patch to the right of the fixation point (the reference) was constant within a session, whereas that of the patch to the left of

the fixation point (the probe) varied from trial to trial. The number of dots in the probe patch was varied according to the QUEST adaptive algorithm (Watson & Pelli, 1983), perturbed by a Gaussian jitter ($\sigma = 0.15$ log units).

Stimuli were generated with the Psychophysics Toolbox (Brainard, 1997) and presented at a viewing distance of 57 cm on a 24-in. LCD monitor (resolution = 1,600 × 1,000 pixels; refresh rate = 60 Hz; mean luminance = 60 cd/m²; Hewlett Packard, Palo Alto, CA). In each stimulus, half of the dots were white, and the other half were black. Each dot had a diameter of 0.3°, and the dots were always separated from each other by at least 0.3°. Dots were randomly displayed within virtual circular patches with a diameter of either 8° or 14°. The patches were centered 13° left or right of fixation. The

Corresponding Author:

David C. Burr, Department of Psychology, University of Florence, Via S. Salvi 12, Pisa 56100, Italy
E-mail: dave@in.cnr.it

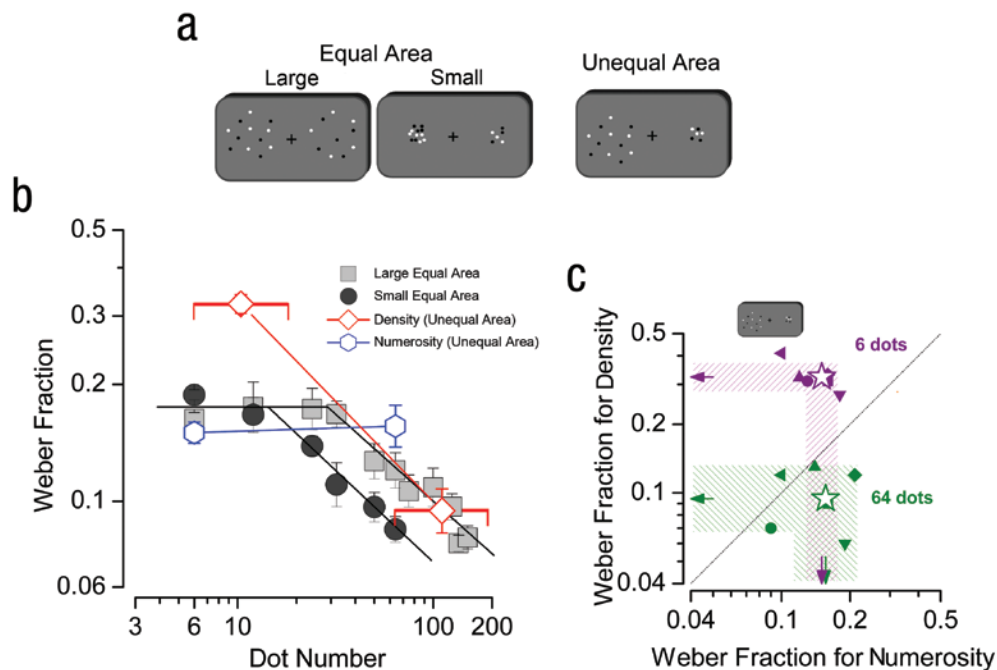


Fig. 1. Experimental stimuli and results. The stimuli (a) were confined to circles with a diameter of either 14° or 8° , centered 13° to either side of a fixation point. In all cases, the reference patch, which contained a constant number of dots, was on the right, whereas the probe patch, which contained a variable number of dots, was on the left. The illustrations show (from left to right) examples of stimuli in the large-equal-area, small-equal-area, and unequal-area conditions. The filled symbols in (b) show Weber fractions (thresholds normalized by perceived number of dots) as a function of dot number in the large-equal-area and small-equal-area conditions. The blue hexagons show thresholds for discriminating numerosity in the unequal-area condition. The red diamonds show thresholds for discriminating density in the same condition. The red horizontal brackets span the range of numerosity of the two patches in the unequal-area condition (more dots in the larger patch); the diamonds are positioned on the geometric mean of these extremes. All thresholds are the geometric means of 6 subjects. Error bars refer to ± 1 SEM. The curves are two-segment, piecewise linear fits of the data, the first of slope zero and the second free to vary. The graph in (c) shows individual subjects' Weber fractions for discriminating density as a function of their Weber fractions for discriminating numerosity in the unequal-area condition (subjects coded by symbol shape), separately for reference patches of 6 dots (purple) and reference patches of 64 dots (green). The striped areas show 95% confidence intervals. The dotted diagonal line is the equithreshold line.

patch with the 8° diameter covered 50 deg^2 , and the patch with the 14° diameter covered 154 deg^2 .

Six subjects with normal or corrected-to-normal vision participated in this study: 2 of the authors and 4 subjects naive to the goals of the study (5 men, 1 woman; mean age = 27 years). At the beginning of each trial, subjects fixated the point in the center of the screen. After a random interval of between 300 and 1,300 ms, the two dot clouds were presented for 240 ms, and subjects were asked to indicate, by pressing a button on a computer keyboard, which cloud was more numerous or more dense.

In the equal-area conditions, the reference and probe patches were the same size, either small (8°) or large (14°). Before formal data collection, subjects were familiarized with these conditions via two 30-trial practice

sessions in which they were given no feedback regarding correct or incorrect responses. We also measured thresholds for patches with different areas (unequal-area condition), in which a small reference patch appeared with a large probe patch. Before data for this condition were collected, all subjects received two training sessions of 50 trials; if the subjects made an error during the training, they heard a feedback tone. The feedback was provided to eliminate the systematic biases in discrimination judgments that have been reported in the literature (Dakin et al., 2011). Because we report Weber fractions rather than coefficients of variation, this seemed to be a sensible precaution.

Two 50-trial sessions (one for numerosity judgments and one for density judgments) were run for each condition. The order of conditions was randomized differently

for different subjects. During the experimental trials, in which no feedback was given, no significant biases were recorded in any of the three conditions.

The proportion of trials in which the probe appeared more numerous or more dense than the reference was plotted against the number of reference dots and fitted with a Gaussian error function. The median of such a function estimates the point of subjective equality, and the standard deviation estimates the precision threshold (i.e., a just-noticeable difference), which was divided by point of subjective equality (a measure of perceived numerosity) to estimate the Weber fraction. We also calculated the coefficient of variation (threshold divided by physical numerosity). However, because this calculation gave results similar to those obtained when we used the median and standard deviation, we decided to stay with the formally correct definition of the Weber fraction.

Results

The filled symbols in Figure 1b plot average Weber fractions (thresholds normalized by perceived numerosity) for numerosity discrimination as a function of number of dots in the reference patch in the equal-area conditions. For both small (8°) and large (14°) patch sizes, thresholds follow Weber's law at low numerosities (constant Weber fraction around 0.18) and then decrease steadily with numerosity, with log-log slopes near 0.5 (square-root relationship). The curves passing through the data points are two-segment, piecewise linear fits of the data, the first of slope zero and the second free to vary. For both large and small reference patches, the best fit of the slope of the second limb was near -0.5 (-0.45 and -0.47 , respectively). The point of slope change for the large reference patch was 29 dots (0.2 dots/deg²), and that for the small reference patch was 14 dots (0.3 dots/deg²). This behavior points to the action of two separate mechanisms, one with thresholds that increase proportionally with numerosity (Weber's law) and another with thresholds that increase with the square root of numerosity. We suggest that the first Weber function reflects the action of number mechanisms, whereas the square-root relationship—which begins to take effect at densities around 0.25 dots/deg²—reflects another system for discriminating density. Because the areas of the two patches were always the same (either both large or both small) in the equal-area conditions, density (numerosity per unit area) necessarily covaried with numerosity, so numerosity and density provided equally valid cues for veridical discrimination (irrespective of the instructions).

The strategy of using density as a proxy for number (and vice versa) is easily thwarted by varying the size of the two comparison patches and then asking subjects to compare the numerosity and, separately, the density of an 8° with that of a 14° patch. Figure 1b shows the results

for discrimination of numerosity for reference numerosities of 6 and 64. Again, Weber's law is observed, and the Weber fraction for the unequal-area condition is similar to that for the equal-area conditions. For the larger numerosity, the Weber fraction was higher for the unequal-area condition than for either of the equal-area conditions, which is consistent with the suggestion that the equal-area conditions can tap different mechanisms, numerosity or density, depending on which is more sensitive. However, at the lower numerosity, thresholds were comparable in the equal- and unequal-area conditions, which shows that unequal area does not necessarily incur a cost for numerosity discrimination (in accordance with the findings of Ross & Burr, 2010).

The results for density discrimination in Figure 1b show a different pattern for the unequal-area condition. At low densities, the Weber fraction is very high (0.3), far higher than in either of the equal-area conditions; at high densities, however, it drops to 0.08, comparable with the Weber fraction for the equal-area condition over this density range. The line connecting these two points has a log-log slope value of 0.51. We predicted that density thresholds would be higher than numerosity thresholds at low numerosities (which would show that the change in slope is not due simply to a saturation effect) and lower than numerosity thresholds at high numerosities, and the results confirmed our predictions.

Figure 1c shows the consistency of the data across subjects. For each subject, the Weber fraction for density discrimination is plotted against the Weber fraction for numerosity discrimination, for both a low and a high numerosity. The Weber fractions for numerosity are clustered around 0.15 for both the 6-dot and the 64-dot conditions; the Weber fractions for density, however, fall into two very distinct clusters that differ by a factor of 3.4. The 95% confidence bands show that the difference between the 6- and 64-dot conditions is highly significant for density discrimination.

Figure 2 shows the predictions of two distinct models of numerosity discrimination. The graph on the left shows the predictions of a model in which estimated number (\hat{N}) is derived from the product of the estimates of density (D) and area (A), as in many theories (e.g., Dakin et al., 2011). If we assume that these estimates are corrupted by independent additive noise (η_D and η_A , respectively), a value for overall noise can be calculated as follows:

$$\hat{N} = (D + \eta_D)(A + \eta_A) \quad (1)$$

$$\hat{N} = DA + \eta_A D + \eta_D A + \eta_D \eta_A \quad (2)$$

If we further assume that area estimation scales with area and is independent of number (but see later in this section), η_A will be constant for constant patch size:

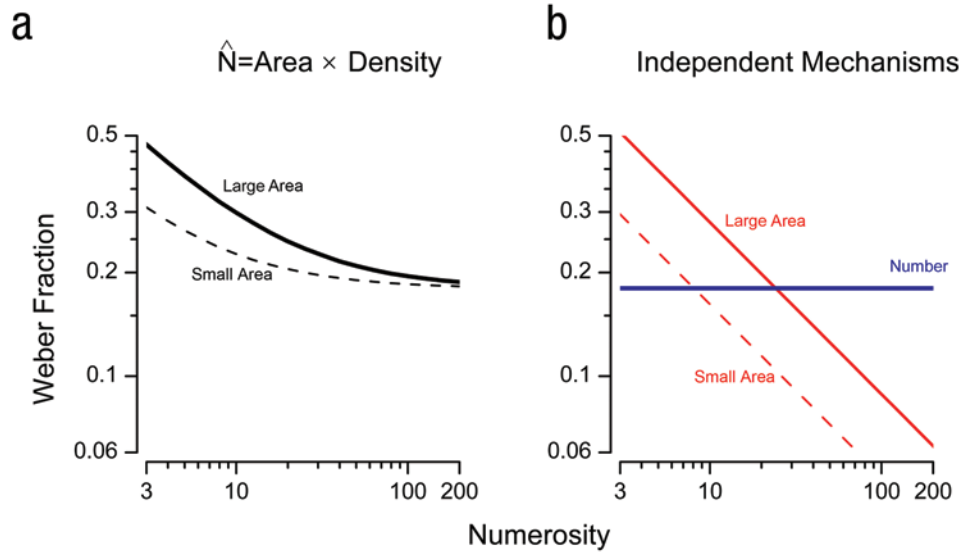


Fig. 2. Two models' predictions of how Weber fractions vary with numerosity in the large-equal-area condition (14°) and the small-equal-area condition (8°). If numerosity is derived from the product of the noisy estimates of area and density (see Equations 1–6 in the text; a), the free parameters k_D and k_A of Equation 6 govern the horizontal and vertical positions, respectively, of the curves. However, our findings predict separate mechanisms (b) for number and density. Numerosity discrimination is assumed to follow Weber's law (Equation 7), and density discrimination to follow Equation 9. The more sensitive mechanism will determine thresholds for any given numerosity.

$$\eta_A = k_A, \quad (3)$$

where k_A is an arbitrary constant.

D and the associated noise, η_D , both depend on number. We assume¹ that density noise increases with the square root of numerosity:

$$\eta_D = k_D \sqrt{N} \quad (4)$$

Substituting Equations 3 and 4 into Equation 2, we obtain the noise for the estimated number:

$$\eta_N = k_D A \sqrt{N} + k_A N + k_A k_D A \sqrt{N} \quad (5)$$

After the negligible term $k_A k_D A \sqrt{N}$ is removed, dividing by N gives the Weber fraction for the product:

$$w_N = \frac{k_D}{\sqrt{N}} A + k_A \quad (6)$$

The trend of this model is clear in Figure 2: For low numerosity (where density noise dominates), Weber fractions decrease with numerosity; the curves then reach asymptotes as area noise begins to dominate at larger numerosities. The height of the function and the position of the asymptote are determined by free parameters k_A and k_D , but the general shape of the function is an

initial decline followed by a plateau. Clearly, this model does not describe the data shown in Figure 1b. Furthermore, it fails to predict the data for the unequal-area condition, in which density cannot be used as a proxy for number, and vice versa. If the computation were always made via density, it would be hard to explain how estimating number or density could lead to such different results.

For simplicity, in constructing the model estimating number from the product of area and density, we assumed that area noise does not depend on numerosity. However, this may not be true because of the greater physical variability in area when the perimeter is constrained by few dots. We simulated a more realistic estimate of area by measuring the *convex hull* (the smallest convex set containing all dots); the variability of these measurements was incorporated into the area noise. The pattern of results was similar; an initial decline in the Weber fraction, followed by a plateau. However, the convex-hull estimates led to even higher Weber fractions at lower numerosities, further still from the actual data trend.

The graph on the right in Figure 2 shows the predictions of a model based on two independent mechanisms, one for numerosity and the other for density. We assume that the noise in estimating number is proportional to number:

$$\sigma_N = w_N, \quad (7)$$

where w_N is the Weber fraction. We again assume (see note 1) that the density noise increases with the square root of numerosity:

$$\sigma_D = k_D \sqrt{N}, \quad (8)$$

where k_D is a constant. Dividing by N gives the Weber fraction for density w_D :

$$w_D = \frac{k_D}{\sqrt{N}} \quad (9)$$

We assume these mechanisms to be independent, so the most sensitive will determine the threshold for any particular numerosity. This simulation clearly captures the trend of the data in Figure 1b for both the large- and the small-equal-area conditions. It also predicts the data for the unequal-area condition, in which density cannot be used as a proxy for number, and vice versa. In the unequal-area condition, the Weber fractions for numerosity follow the numerosity curve in the right-hand graph in Figure 2, and the Weber fractions for density follow the density curve.

Discussion

In the past, the presence of two distinct psychophysical laws governing thresholds has often been taken to imply two distinct neural mechanisms. Perhaps the most famous example is the time course of recovery from dark adaptation, in which the initial rapid recovery is taken to reflect the action of cones, whereas the later slower recovery is taken to reflect the action of rod cells in the retina (Hecht, 1921). Likewise, we suggest, the two distinct limbs governing numerosity thresholds reflect two distinct mechanisms.

Numerosity can be defined as the product of density and area, which implies that the nervous system calculates it in that way. For example, although velocity equals displacement divided by time, the system need not compute displacement and time separately and perform the division. It is well known that the speed and direction of objects in motion are detected by dedicated mechanisms, and sensitivity to motion is far greater than that which could be obtained from independent estimates of space and time (e.g., Burr & Ross, 1986). Likewise, it seems that the visual system senses numerosity directly (for relatively low densities, at least) without requiring estimates of density or area.

Weber's law for numerosity is consistent with many previous observations in both humans and other animals (Nieder, 2005; Ross, 2003; Whalen, Gallistel, & Gelman, 1999) and is well predicted by the logarithmic bandwidth

of neurons selective for number (Nieder, 2005). The mechanisms that come into play for density discriminations are unclear, but it is not unreasonable to assume that density is based on average dot separation. However, the exact manner by which average nearest-neighbor distance is decoded to yield estimates of density goes beyond the scope of this study.

Whatever the exact mechanisms behind coding of number and density, the distinct psychophysical curves describing thresholds for high and low densities in the equal-area conditions (in which density and numerosity provide equivalent information) point to two separate mechanisms. This suggestion was supported by the data from the unequal-area-condition (variable patch size), which thwarted the strategy of switching mechanisms to optimize performance: Weber fractions for numerosity were the same for large and small numbers, whereas those for density varied by a factor of 3.4 for a 10-fold change in number, which is again consistent with the square-root law. This result finds support in many studies, including those showing that apparent numerosity depends strongly on luminance, whereas texture density does not (Ross & Burr, 2010), and that many manipulations that affect discrimination of numerosity do not affect discrimination of density. Linking neighboring points of a random-dot display greatly reduces apparent number without increasing density judgments (Franconeri, Bernis, & Alvarez, 2009; He, Zhang, Zhou, & Chen, 2009). However, such findings are inconsistent with suggestions that a common mechanism underlies both density and numerosity discrimination or that perceived numerosity is derived only from density (Dakin et al., 2011).

Author Contributions

G. Anobile, G. M. Cicchini, and D. C. Burr devised the experiment. G. Anobile and G. M. Cicchini collected and analyzed the data. D. C. Burr performed the modeling. All authors wrote the manuscript.

Declaration of Conflicting Interests

The authors declared that they had no conflicts of interest with respect to their authorship or the publication of this article.

Funding

This work was supported by the Space, Time, and Number in the Brain (STANIB) program of the European Research Council under the European Union's Seventh Framework Programme for Research (FP7) and by the Italian Ministry of Research.

Note

1. We verified this assumption by running a Monte Carlo simulation based on nearest-neighbor distances. For each dot, we calculated the average distance of the four nearest neighbors; we then averaged this distance over all dots within a given area. We

compared two such independent averages 2,000 times to obtain simulated psychometric functions. The standard deviation of the Gaussian error function fitting these data increased with \sqrt{N} over the range of numerosities of our study, as assumed in Equation 4.

References

- Brainard, D. H. (1997). The Psychophysics Toolbox. *Spatial Vision, 10*, 433–436.
- Burr, D., & Ross, J. (2008a). A visual sense of number. *Current Biology, 18*, 425–428.
- Burr, D., & Ross, J. (2008b). Response: Visual number [Letter]. *Current Biology, 18*, R857–R858.
- Burr, D. C., & Ross, J. (1986). Visual processing of motion. *Trends in Neurosciences, 9*, 304–307.
- Dakin, S. C., Tibber, M. S., Greenwood, J. A., Kingdom, F. A., & Morgan, M. J. (2011). A common visual metric for approximate number and density. *Proceedings of the National Academy of Sciences, USA, 108*, 19552–19557.
- Dehaene, S. (1997). *The number sense: How the mind creates mathematics*. New York, NY: Oxford University Press.
- Durgin, F. H. (2008). Texture density adaptation and visual number revisited [Letter]. *Current Biology, 18*, R855–R856.
- Franconeri, S. L., Bemis, D. K., & Alvarez, G. A. (2009). Number estimation relies on a set of segmented objects. *Cognition, 113*, 1–13.
- He, L., Zhang, J., Zhou, T., & Chen, L. (2009). Connectedness affects dot numerosity judgment: Implications for configural processing. *Psychonomic Bulletin & Review, 16*, 509–517.
- Hecht, S. (1921). The nature of foveal dark adaptation. *Journal of General Physiology, 4*, 113–139.
- Nieder, A. (2005). Counting on neurons: The neurobiology of numerical competence. *Nature Reviews Neuroscience, 6*, 177–190.
- Ross, J. (2003). Visual discrimination of number without counting. *Perception, 32*, 867–870.
- Ross, J., & Burr, D. C. (2010). Vision senses number directly. *Journal of Vision, 10*(2), Article 10. Retrieved from <http://www.journalofvision.org/content/10/2/10>
- Watson, A. B., & Pelli, D. G. (1983). QUEST: A Bayesian adaptive psychometric method. *Perception & Psychophysics, 33*, 113–120.
- Whalen, J., Gallistel, C. R., & Gelman, R. (1999). Nonverbal counting in humans: The psychophysics of number representation. *Psychological Science, 10*, 130–137.